Interdependence of the Hammett and isokinetic relationships: a numerical simulation approach

Joaquin F. Perez-Benito[1] iD **● Arnau Clavero-Masana[1]**

Received: ……/Accepted …

Abstract

Many homologous reaction series present linear correlations between the enthalpy ($\Delta H^{o}_{\neq,i}$) and entropy ($\Delta S^{o}_{\neq,i}$) of activation (kinetic compensation effect), the slope being the isokinetic temperature of the series (T_{iso}), so that at $T = T_{iso}$ all the reactions of the family share the same value of the rate constant. However, the random errors committed in the laboratory in the determination of $\Delta H^{o}_{\neq,i}$ and $\Delta S^{o}_{\neq,i}$ are interrelated, and so tend to produce false isokinetic relationships. As a result, the existence of physically meaningful isokinetic relationships is a topic of lasting controversy. Here it is shown that both the LFER (linear free energy relationships)-type and isokinetic linear correlations are direct consequences of two other correlations, those of $\Delta H^{o}_{\neq,i}$ vs. σ_i and $\Delta S^{o}_{\neq,i}$ vs. σ_i, where the abscissa is the Hammett (or Taft) substituent parameter. A mathematical model has been developed, according to which T_{iso} can be interpreted as the temperature at which the reaction constant obtained as the slope of the LFER-type straight line takes a zero value ($\rho = 0$). Moreover, the

numerical simulations performed indicated that the $\log k_T$ vs. σ_i and $\Delta H^o_{\neq,i}$ vs. $\Delta S^o_{\neq,i}$ linear plots can be visualized as two faces of the same coin, since, if the kinetic data obey the first with a correlation coefficient high enough, the probability of fulfillment of the second will be very high. Finally, it has been found that values of T_{iso} and T_δ (the slope of the linear correlation between the enthalpy-entropy deviations) very close to the mean working temperature, as well as correlation coefficients of the $\Delta H^o_{\neq,i}$ vs. $\Delta S^o_{\neq,i}$ linear plots much higher than those corresponding to the $\Delta H^o_{\neq,i}$ vs. σ_i and $\Delta S^o_{\neq,i}$ vs. σ_i plots, are all indicative of false isokinetic relationships, highly contaminated by the statistical correlation between the enthalpy and entropy experimental errors.

Keywords Computational chemistry ● Hammett relationship ● Isokinetic relationship ● Kinetics ● Semiempirical calculations

✉ Joaquin F. Perez-Benito
jfperezdebenito@ub.edu

[1] Departamento de Ciencia de Materiales y Quimica Fisica, Seccion de Quimica Fisica, Facultad de Quimica, Universidad de Barcelona, Marti i Franques 1, 08028 Barcelona, Spain

Introduction

It is a common practice in the chemical kinetics laboratory to study what are known as homologous reaction series, understanding for that term families of closely related chemical processes differing, for instance, either in the structure of one of the reactants (replacing an inert substituent with another) [1–4] or in the solvent employed [4, 5].

A surprising result often found in these studies is the existence of a compensation effect, because when the activation enthalpy increases along the reaction series (unfavorable effect on the reaction rate) the activation entropy increases too (favorable effect). Moreover, the compensation may be complete at a certain temperature provided that there is a linear correlation between the activation parameters obtained for each member (i) of the reaction family:

$$\Delta H^{\circ}_{\neq,\mathrm{i}} = \Delta H^{\circ}_{\neq,\mathrm{h}} + T_{\mathrm{iso}}\,\Delta S^{\circ}_{\neq,\mathrm{i}} \qquad (1)$$

where $\Delta H^{\circ}_{\neq,\mathrm{h}}$ is the value of the activation enthalpy for a hypothetical reaction (h) of the series with $\Delta S^{\circ}_{\neq,\mathrm{i}} = 0$ and T_{iso} is the parameter known as isokinetic temperature of the set of chemical processes under consideration. This magnitude receives its name from the fact that when the experiments are performed at the temperature $T = T_{\mathrm{iso}}$ all the reactions share the rate constant:

$$k_{\mathrm{iso}} = \frac{k_{\mathrm{B}}\,T_{\mathrm{iso}}}{h}\,(c^{\circ})^{1-n}\,e^{-\frac{\Delta H^{\circ}_{\neq,\mathrm{h}}}{RT_{\mathrm{iso}}}} \qquad (2)$$

where k_B, h and R are the Boltzmann, Planck and ideal gas constants, respectively, c^o = 1 mol L^{-1} the standard concentration and n the kinetic order. This rate constant value would be the same for all the chemical processes of the series, since the intercept ($\Delta H^o_{\neq,h}$) and slope (T_{iso}) of the linear compensation plot ($\Delta H^o_{\neq,i}$ vs. $\Delta S^o_{\neq,i}$) remain invariable throughout the reaction family.

The observation of enthalpy-entropy linear relationships of the kind shown in Eq. (1) is rather overwhelming, not only in the field of chemical kinetics (determination of rate constants [6–8]) but also in those of chemical thermodynamics (determination of equilibrium constants [9]), surface chemistry (determination of adsorption parameters [10]), physics (determination of gas-liquid absorption parameters [11, 12], viscosities [13], diffusion coefficients [14–17], polymer relaxation frequencies [18], silicon annealing rates [19], crystal growth rates [20], semiconductor thermal electron emission rates [21] or solid-state electrical conductivities [22–28]) and even food technology [29]. However, its acceptance as a physically meaningful phenomenon remains considerably controversial [30–34]. This is so because of the fact that the simultaneous determination of the enthalpy and entropy from the same fit makes their respective experimental imprecisions interdependent [35–37], random [38, 39] and systematic [40] errors being thus responsible for at least many of the observed compensation plots.

However, for some homologous reactions series the evidences supporting the existence of an isokinetic behavior are strong enough so as not to be easily discarded as error-driven artifacts [41, 42]. Different theoretical explanations have been proposed to uncover the roots of the compensation effect at the physicochemical level [43], such as the selective energy transfer model [44–48] or the multi-excitation entropy model [49–52].

In the present work, it will be defended that the enthalpy-entropy compensation effect (either physical or chemical) is in all likelihood a multifactorial phenomenon, and several potential causes are probably involved. Indeed, experimental errors constitute one of those causes, but they should not be considered as the only exclusive one. To this respect, and in order to clarify another of the possible causes, a chemical-approach model, based on the electronic effects modulating reactivity, will be considered and confronted with the experimental information available.

One of the conclusions that can be reached from that model is the close proximity of the Hammett/Taft and activation enthalpy-entropy linear plots for a certain homologous reaction series. Actually, the interrelation between the LFER-type and isokinetic relationships has previously been reported and discussed by other authors [53, 54]. The results from some numerical simulation studies will now be provided to support this conclusion.

Results and Discussion

LFER-type relationships and kinetic compensation effect

An isokinetic model (of a strictly chemical nature) can be developed taking as a basis the correlations of the LFER (linear free energy relationships) type. Let us start by considering a homologous reaction series that follows either the Hammett or the Taft equation irrespectively of temperature (within a certain range). In the hypothetical case chosen as an example, the reaction constant (slope of the LFER-type plot) is negative (ρ or ρ^* < 0), corresponding to a favorable effect of the electron-donating substituents [55, 56], whereas a positive value (ρ or ρ^* > 0) would correspond to a favorable effect of the electron-withdrawing substituents [57, 58].

As can be observed (Fig. 1, top), provided that the reaction constant of the family changes with temperature, there will necessarily be a crossing point between the log k vs. σ (or σ*) straight lines associated with two different temperatures (where σ and σ* are the Hammett and Taft substituent parameters, respectively). That point corresponds evidently to a reaction of the series (either real or hypothetical) with a zero value of the activation energy (E_a = 0), and hence with a temperature-independent rate constant, so that the straight lines for other temperatures will pass through the same point, yielding a common intersection of all the Hammett (or Taft) linear plots.

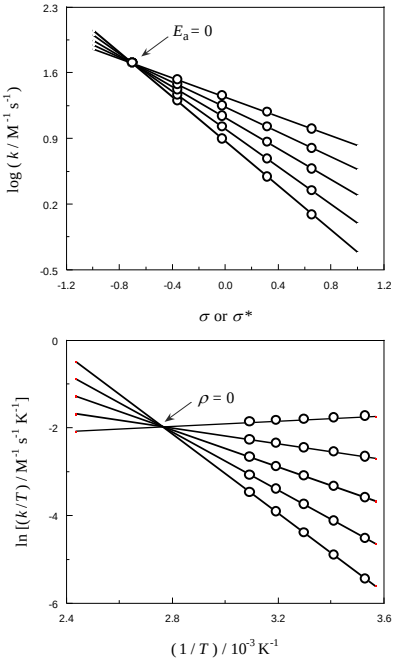

Fig. 1 Simulated plots for a second-order homologous reaction series with the activation energies (0, 10, 20, 30 and 40) kJ mol^{-1} at the temperatures (10, 20, 30, 40 and 50) ºC. Top: Hammett or Taft plots (the circles correspond to the different activation energies and the straight lines to the temperatures). Bottom: Eyring plots (the circles correspond to the different temperatures and the straight lines to the activation energies)

On the other hand, provided that the activation energy changes from one member of the family to another, there will necessarily be a crossing point between the ln (k/T) vs. $1/T$ straight lines (Eyring plots) associated with two different reactions. That point corresponds evidently to a temperature (extrapolated) at which the reaction constant would equal zero (ρ or ρ* = 0), and hence with a rate constant independent of the electronic effects provoked by the substituents, so that the straight lines for other reactions will pass

through the same point, yielding a common intersection of all the Eyring linear plots (Fig. 1, bottom).

Moreover, from the Arrhenius, Eyring and Hammett equations it follows rather straightforwardly that:

$$\Delta H^{o}_{\neq,i} = T_{iso} \left[R \ln \frac{k_B T_{iso} (c^o)^{1-n}}{h A_{\sigma_{iso}}} + \Delta S^{o}_{\neq,i} \right] \quad (3)$$

where σ_{iso} is the Hammett substituent parameter for a hypothetical reaction with zero activation energy and $A_{\sigma_{iso}}$ the corresponding Arrhenius pre-exponential factor. It can thus be concluded that, if a certain homologous reaction series fulfills both an LFER-type and the Arrhenius (or Eyring) correlations, it will also fulfill the enthalpy-entropy isokinetic correlation.

Temperature dependence of the reaction constant

Now, we will assume that both the enthalpy and entropy of activation must follow linear dependences on the Hammett (or Taft) substituent parameter if the LFER-type correlations are to be fulfilled:

$$\Delta H^{o}_{\neq,i} = A_H + B_H \sigma_i \quad (4)$$

$$\Delta S^{o}_{\neq,i} = A_S + B_S \sigma_i \quad (5)$$

where A_H and A_S are the enthalpy and entropy of activation for a member of the homologous reaction series with $\sigma_i = 0$, respectively, whereas B_H and B_S are the slopes of the corresponding linear plots. Equations (4) and (5) are in complete agreement with experimental data concerning a reaction series fulfilling both the Hammett and isokinetic correlations, the oxidation of *m*- and *p*-substituted cinnamic acids by tributylmethylammonium permanganate in methylene chloride solutions (Fig. 2) [59].

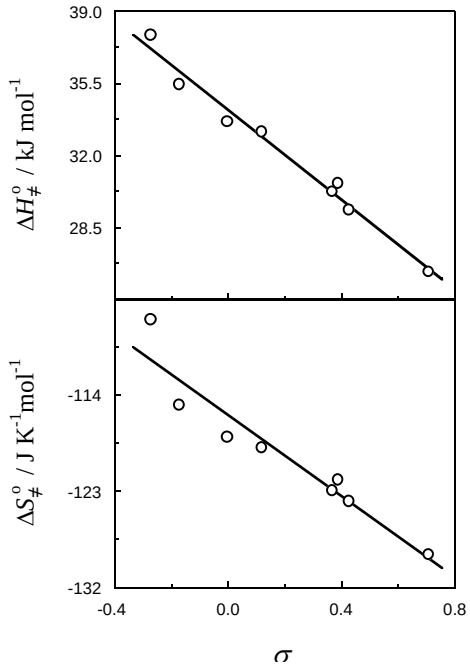

Fig. 2 Experimental enthalpies (r = 0.991, top) and entropies (r = 0.956, bottom) of activation as a function of the Hammett σ parameter for the oxidation of a series of eight *m*- and *p*-substituted cinnamic acids by tributylmethylammonium permanganate in methylene chloride solutions

Replacing into the Eyring equation and writing the Hammett equation as:

$$\log k_{\mathrm{T,\,i}} = \log k_{\mathrm{T,\,H}} + \rho_{\mathrm{T}}\,\sigma_{\mathrm{i}} \tag{6}$$

it follows that Eq. (6) arises from Eqs. (4) and (5) with:

$$k_{\mathrm{T,\,H}} = \frac{k_{\mathrm{B}}T}{h}(c^{\mathrm{o}})^{1-n}e^{\frac{A_{\mathrm{S}}}{R}}e^{-\frac{A_{\mathrm{H}}}{RT}} \tag{7}$$

$$\rho_{\mathrm{T}} = \frac{1}{2.303\,R}\left(B_{\mathrm{S}} - \frac{B_{\mathrm{H}}}{T}\right) \tag{8}$$

so that the reaction constant should present a linear dependence with the reciprocal temperature, either increasing (if $B_{\mathrm{H}} < 0$, Fig. 3, top) or decreasing (if $B_{\mathrm{H}} > 0$, Fig. 3, bottom), in full agreement with the experimental data [59, 60].

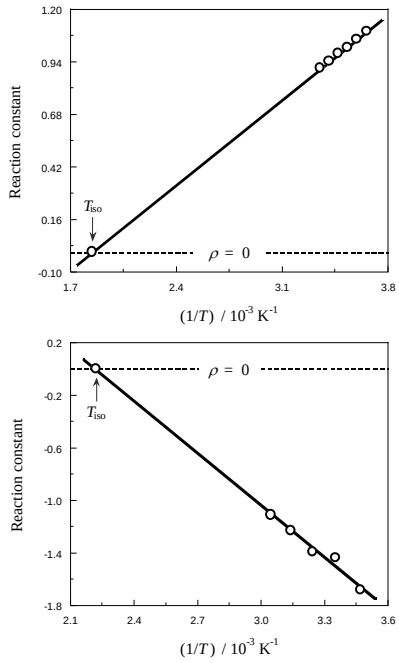

Fig. 3 Experimental values of the Hammett reaction constant as a function of the reciprocal absolute temperature for the oxidation of a series of eight *m*- and *p*-substituted cinnamic acids by tributylmethylammonium permanganate in methylene chloride solutions (T_{iso} = 542 K, top) and the S_NAr reactions of a series of five *m*- and *p*-substituted anilines with 2,6-

bis(trifluoromethanesulfonyl)-4-nitroanisole in methanol solutions (T_{iso} = 450 K, bottom), showing the extrapolation required to reach the respective isokinetic temperatures (ρ = 0)

Moreover, given that according to the present model T_{iso} is the value of the temperature at which the reaction constant equals zero (the electron density of the functional group has no effect on the reaction rate), we can write for the isokinetic temperature of the homologous series:

$$T_{iso} = \frac{B_H}{B_S} \quad (9)$$

In fact, it is easy to see that the isokinetic correlation, Eq. (1), arises from Eqs. (4) and (5), the intercept being $\Delta H^{o}_{\neq,h} = (A_H B_S - B_H A_S)/B_S$ and the slope being given by Eq. (9).

Numerical simulations: one activation parameter scattered

This first type of simulations was carried out assuming either that he $\Delta H^{o}_{\neq,i}$ vs. σ_i was a perfect straight line and the entropies were scattered according to the equation:

$$\Delta S^{o}_{\neq,i,sim} = \left(A_S + B_S \sigma_i\right)\left(1 + \frac{F R}{1000}\right) \quad (10)$$

where parameters A_S and B_S were obtained from the fitting of the experimental activation entropies to Eq. (5) or, else, that the $\Delta S^{o}_{\neq,i}$ vs. σ_i was a perfect straight line and the enthalpies were scattered according to the equation:

$$\Delta H^{o}_{\neq,i,sim} = \left(A_H + B_H \sigma_i\right)\left(1 + \frac{F R}{1000}\right) \quad (11)$$

where parameters A_H and B_H were obtained from the fitting of the experimental activation enthalpies to Eq. (4), whereas the dispersion factor took values in the $0 < F < 100$ % range, and the random numbers in the $-10 < R < +10$ range.

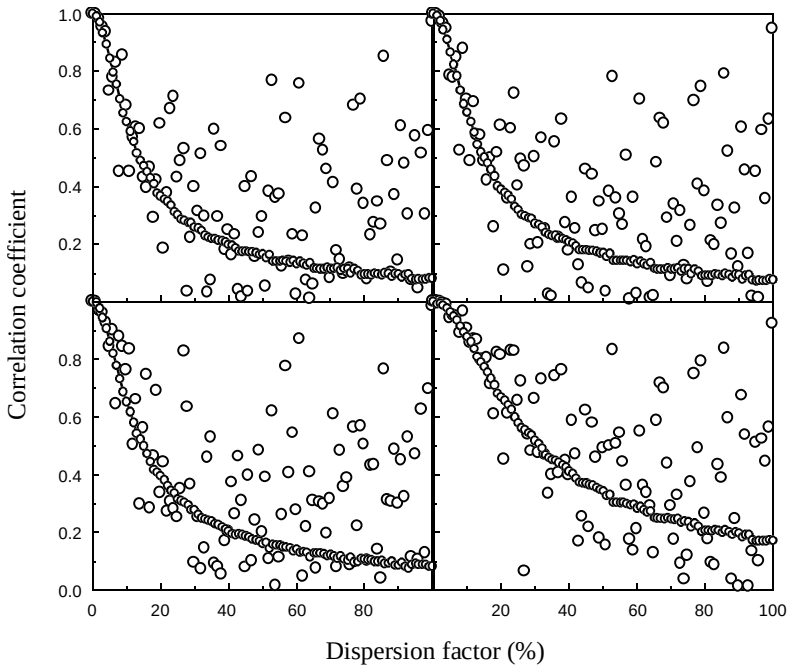

Fig. 4 Linear correlation coefficients associated with the $\log k_{298,i}$ vs σ_i (top) and $\Delta H^{o}_{\neq,i}$ vs. $\Delta S^{o}_{\neq,i}$ (bottom) plots as a function of the dispersion factor from simulations based on the oxidation of a series of eight *m*- and *p*-substituted cinnamic acids by

tributylmethylammonium permanganate in methylene chloride solutions, assuming that only either the entropies (left) or the enthalpies (right) of activation were dispersed, showing the scattered points found when the simulations were performed just once and the maximum probability curves found when the simulations were performed 10^6 times for each *F* value

Some of the results obtained are shown in Fig. 4, including the scattered points obtained when the simulations were performed just once and the well-behaved maximum probability curves obtained from the average data corresponding to 10^6 simulations for each *F* value.

We can see that the dependences of the correlation coefficients corresponding to the $\log k_{298,\mathrm{i}}$ vs. σ_{i} and $\Delta H^{\mathrm{o}}_{\neq,\mathrm{i}}$ vs. $\Delta S^{\mathrm{o}}_{\neq,\mathrm{i}}$ linear plots on the value of the dispersion factor followed similar patterns. Actually, when only the activation entropies were scattered, the correlation coefficients of the Hammett and isokinetic relationships were very similar. Nevertheless, when the scattered parameters were the activation enthalpies, the correlation coefficient of the isokinetic relationship was clearly higher than that of an LFER kind of correlation. This difference might have a mathematical origin rather than a physically meaning one, since it seems to be related to the fact that, when only the activation enthalpies are dispersed, at high dispersion factor values the slope of the $\Delta H^{\mathrm{o}}_{\neq,\mathrm{i}}$ vs. $\Delta S^{\mathrm{o}}_{\neq,\mathrm{i}}$ linear plot tends to be also high, so that

the errors of the ordinates with respect to the straight line become less important.

Numerical simulations: both activation parameters scattered

The simulations of this last class of trials were implemented assuming this time that both the enthalpies and entropies of activation were scattered, according to Eqs. (10) and (11). In order to avoid the statistical error correlation between the enthalpy and entropy values, the random numbers R involved in Eq. (11) were independent of those involved in Eq. (10). The results obtained are shown in Fig. 5 (comparison of the maximum probability curves corresponding to the $\Delta H^{o}_{\neq,i}$ vs. σ_i, $\Delta S^{o}_{\neq,i}$ vs. σ_i, $\log k_{298,i}$ vs. σ_i and $\Delta H^{o}_{\neq,i}$ vs. $\Delta S^{o}_{\neq,i}$ linear plots).

It can be seen that the correlation coefficients associated to the four plots followed parallel patterns. In particular, the correlation coefficients of the Hammett and isokinetic plots were very similar, one of them (isokinetic) being higher in the range $0 < F < 23$ % and the other (Hammet) being higher in the range $23 < F < 100$ %. This seems to suggest that the linearity of both the $\Delta H^{o}_{\neq,i}$ vs. σ_i and $\Delta S^{o}_{\neq,i}$ vs. σ_i plots constitutes an important condition for the $\log k_{298,i}$ vs. σ_i (Hammett) and $\Delta H^{o}_{\neq,i}$ vs. $\Delta S^{o}_{\neq,i}$ (isokinetic) plots being simultaneously linear.

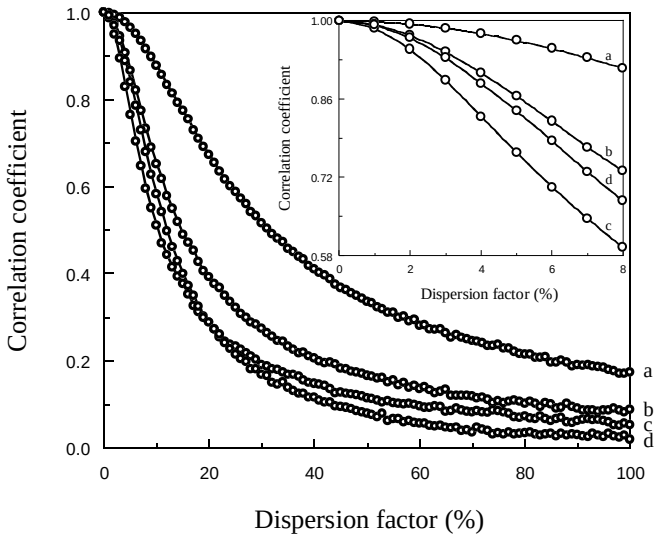

Fig. 5 Linear correlation coefficients associated with the $\Delta H^{o}_{\neq,i}$ vs. σ_i (a), $\Delta S^{o}_{\neq,i}$ vs. σ_i (b), $\log k_{298,i}$ vs. σ_i (c) and $\Delta H^{o}_{\neq,i}$ vs. $\Delta S^{o}_{\neq,i}$ (d) plots as a function of the percent dispersion factor from numerical simulations based on the oxidation of a series of eight *m*- and *p*-substituted cinnamic acids by tributylmethylammonium permanganate in methylene chloride solutions, showing the maximum probability curves found when the simulations were performed 10^4 times for each *F* value. Inset: detail showing the range $F = 0 - 8$ %

In order to advance more deeply in the knowledge of the interconnections existing between the Hammett and isokinetic relationships, we have calculated the probability of both being simultaneously linear for different values of the dispersion factor (performing 10^6 numerical simulations for each value) and plotted the results against the probability of the Hammett relationship (considered independently of the other) being linear (Fig. 6, top).

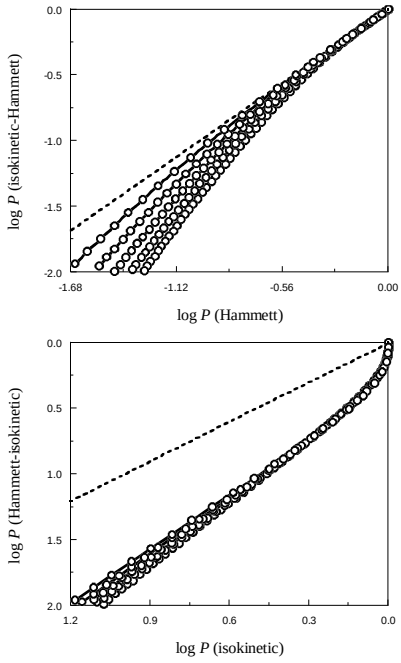

Fig. 6 Top: double logarithm plots of the probability of the $\Delta H^{o}_{\neq,i}$ vs. $\Delta S^{o}_{\neq,i}$ and $\log k_{298,i}$ vs. σ_i relationships being simultaneously linear as a function of the probability of the $\log k_{298,i}$ vs. σ_i relationship considered alone being linear. Bottom: double logarithm plots of the probability of the $\log k_{298,i}$ vs. σ_i and $\Delta H^{o}_{\neq,i}$ vs. $\Delta S^{o}_{\neq,i}$ relationships being simultaneously linear as a function of the probability of the $\Delta H^{o}_{\neq,i}$ vs. $\Delta S^{o}_{\neq,i}$ relationship considered alone being linear. From 10^6 numerical simulations performed for each *F* value, based on the cinnamic acid reaction series, with dispersion factor values in the range $F = 0.0 - 7.2$ % and correlation coefficients higher than 0.90, 0.92, 0.94, 0.96 and 0.98 (in upward order). The dashed lines correspond to a condition for which the two probabilities would be identical

It can be seen that, although the probability of simultaneous isokinetic-Hammett linearity was indeed lower than that corresponding to the Hammett

relationship considered alone, both of them approached the same limit value when the required correlation coefficient increased:

$$\lim_{r \to 1} P\,(\text{isokinetic-Hammett}) = P\,(\text{Hammett}) \qquad (12)$$

as confirmed by the fact that the straight line $y = x$ (corresponding to identical values of the two probabilities) was tangent to the downward-concave simulation plots.

However, the situation was not symmetrical. Actually, when the calculations were repeated in a reversed way, and the probability of the Hammett and isokinetic relationships being simultaneously linear was plotted against the probability of the isokinetic relationship (considered alone) being linear, the straight line $y = x$ was not tangent to the (this time upward-concave) simulation plots (Fig. 6, bottom). Therefore, an equation equivalent to Eq. (12) was not applicable any longer, meaning that although a good fulfillment of the Hammett correlation implied a good fulfillment of the isokinetic correlation, the converse statement was not true. This means that the requirements for an LFER-type of correlation to be fulfilled are stricter than those for the enthalpy-entropy correlation, probably because the dispersion effect caused on the isokinetic plots when the deviations of the enthalpy and entropy of activation are large is partially compensated as far as the correlation coefficient is concerned, since the slope (T_{iso}) tends also to be large. Since the numerical

simulations were performed so that the dispersion of the activation enthalpy values was independent from that of the activation entropy values, this result should be attributed to the deviations coming from the very own nature of each member of the reaction series rather than to those coming from the experimental errors. In a real case, due to the entanglement of the random errors associated to the enthalpy and entropy of activation, the isokinetic correlation is expected to be even more favored with respect to the Hammett correlation than found in the present simulations.

Hence, the numerical simulations carried out in the present work allow to conclude that the linearity of the LFER-type plots and that of the compensation-type plots are in all likelihood inexorably bounded: the fulfillment of the Hammett (or Taft) correlation for a particular homologous reaction series implies the fulfillment of the isokinetic correlation.

Reproducing the experimental parameters

The average ordinate fitting errors associated with the Hammett (E_{Ham}) and isokinetic (E_{iso}) linear plots were defined from the absolute values of the deviations of the experimental values of the logarithms of the rate constants or the activation enthalpies with respect to those calculated from the best adjusting straight lines as obtained by means of the least square method:

$$E_{\text{Ham}} = \frac{\sum_{i=1}^{N} \left| \log k_{i,\text{exp}} - \log k_{i,\text{cal}} \right|}{N} \quad (13)$$

$$E_{\text{iso}} = \frac{\sum_{i=1}^{N} \left| \Delta H^{o}_{\neq,i,\text{exp}} - \Delta H^{o}_{\neq,i,\text{cal}} \right|}{N} \quad (14)$$

where N is the number of reactions of the homologous series under study.

On the other hand, we will focus our attention now on the number of simulations leading to linear plots close enough to the experimental ones. The simulations accepted as valid were those leading to statistical parameters (slopes and average ordinate fitting errors) within a ten percent margin of the experimental values, ρ = 0.911 and E_{Ham} = 0.0409:

$$0.9\,(\rho)_{\text{exp}} \leq (\rho)_{\text{sim}} \leq 1.1\,(\rho)_{\text{exp}} \quad (15)$$

$$0.9\,(E_{\text{Ham}})_{\text{exp}} \leq (E_{\text{Ham}})_{\text{sim}} \leq 1.1\,(E_{\text{Ham}})_{\text{exp}} \quad (16)$$

in the case of the Hammett plot, or T_{iso} = 542 K and E_{iso} = 0.565 kJ mol^{-1}:

$$0.9\,(T_{\text{iso}})_{\text{exp}} \leq (T_{\text{iso}})_{\text{sim}} \leq 1.1\,(T_{\text{iso}})_{\text{exp}} \quad (17)$$

$$0.9\,(E_{\text{iso}})_{\text{exp}} \leq (E_{\text{iso}})_{\text{sim}} \leq 1.1\,(E_{\text{iso}})_{\text{exp}} \quad (18)$$

in the case of the isokinetic plot (for the cinnamic acid reaction family).

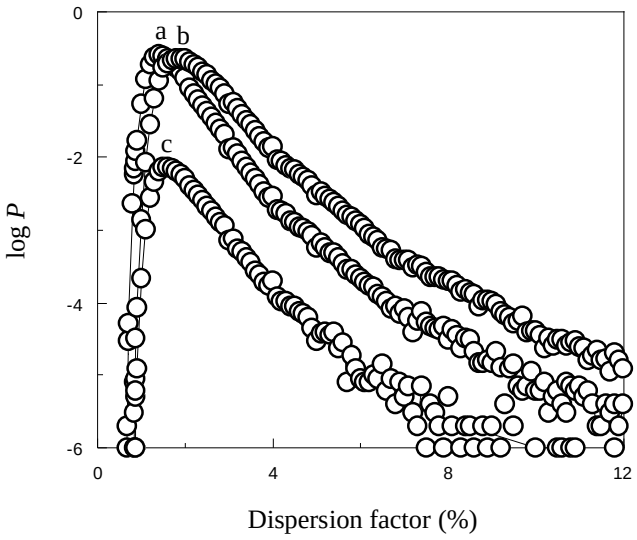

Fig. 7 Logarithm of the probability of the slopes (ρ or T_{iso}) and average ordinate fitting errors (E_{Ham} or E_{iso}) corresponding to the $\log k_{298,i}$ vs. σ_i (a), $\Delta H^{o}_{\neq,i}$ vs. $\Delta S^{o}_{\neq,i}$ (b) or both (c) linear plots being within ± 10 % of the experimental values as a function of the percent dispersion factor, with only the activation entropies scattered, from 10^6 numerical simulations for each F value and based on the oxidation of a series of eight *m*- and *p*-substituted cinnamic acids by tributylmethylammonium permanganate in methylene chloride solutions

The resulting probability curves are shown in Fig. 7 (only the activation entropies scattered) and the coordinates of the respective maxima in Table 1 (all three methods considered).

Table 1 Coordinates of the probability curve maxima[a]

Linear plot	$F_{max,1}$ (%)[b]	$P_{max,1}$[b]	$F_{max,2}$ (%)[c]	$P_{max,2}$[c]	$F_{max,3}$ (%)[d]	$P_{max,3}$[d]
Hammett	1.41	0.263	1.62	0.226	1.12	0.230
Isokinetic	1.88	0.230	3.70	0.192	1.66	0.220
Hammett-Isokinetic	1.56	0.007	—	—	1.80	0.003

[a]From 10^6 numerical simulations for each F value, based on the oxidation of a series of eight *m*- and *p*-substituted cinnamic acids by tributylmethylammonium permanganate in methylene chloride solutions. F_{max} and P_{max} are the abscissa and ordinate values corresponding to the maxima of the probability curves

[b]Method 1: only the activation entropies scattered

[c] Method 2: only the activation enthalpies scattered (P_2 = 0 for the combined Hammett-isokinetic probability curve at all F values)

[d]Method 3: both activation parameters scattered

It can be observed that, when the $\Delta S^{o}_{\neq,i}$ vs. σ_i plot was assumed to be a perfect straight line and the $\Delta H^{o}_{\neq,i}$ values were scattered, none of the 10^6 simulations performed for each F value fulfilled simultaneously the four conditions imposed by Eqs. (29)-(32). This was so because the values of F_{max} associated with the Hammett and isokinetic linear plots were much too different in this case. Actually, the best results were found when only the entropy values were scattered.

Isokinetic temperature: finding the highest probability value

An increase of the dispersion factor led to a decrease of the isokinetic temperature. In order to find a better value of the latter (free from the distortion provoked by the scattering of the experimental data), the maximum probability curve was moved until it matched the experimental point, defined in the T_{iso} vs. $E(T_{iso})$ diagram by its coordinates T_{iso} = 542 K and $E(T_{iso})$ = 43 K (for the cinnamic acid reaction family). This objective was achieved by changing systematically the slope of the $\Delta S^{o}_{\neq,i}$ vs. σ_i plot (the experimental activation entropies were more error prone than the activation enthalpies). It should be noticed that, due to the initial increase and posterior decrease of the isokinetic temperature standard deviation as parameter F increased, a T_{iso} vs. $E(T_{iso})$ plot showed a parabolic profile (Fig. 8, top).

This procedure was applied again taking now as abscissas either the correlation coefficient (Fig. 8, middle) or the average ordinate fitting error (Fig. 8, bottom) of the enthalpy-entropy linear plots, the experimental point being defined in these diagrams by the coordinates T_{iso} = 542 K and either r = 0.981 or E_{iso} = 0.565 kJ mol^{-1}, respectively.

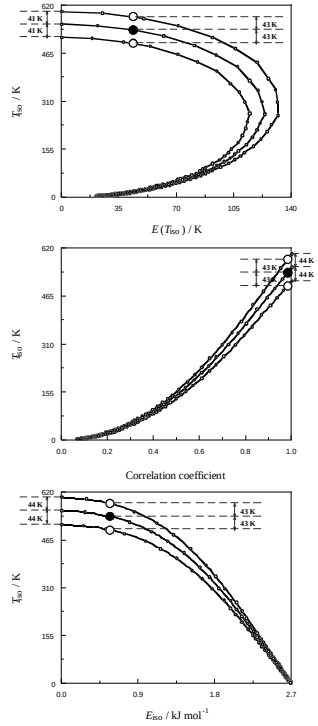

Fig. 8 Isokinetic temperature as a function of either its standard deviation (top), the correlation coefficient (middle) or the average ordinate fitting error (bottom) found when the simulations were performed 10^6 times for each dispersion factor value (in the range $F = 0 - 100$ %) with only the entropies scattered, and based on the oxidation of a series of eight *m*- and *p*-substituted cinnamic acids by tributylmethylammonium permanganate in methylene chloride solutions, showing the maximum probability curves starting at either T_{iso} = (518, 560 and 601) K (top), T_{iso} = (515, 559 and 603) K (middle) or T_{iso} = (516, 561 and 605) K (bottom), as well as the experimental points (filled circles) and their error-tolerated limits (empty circles)

Moreover, since the imprecision associated with the experimental value of the isokinetic temperature was known (± 43 K), the repetition of the method with the limit values allowed to the ordinate (499 and 585 K) led to the errors

of the extrapolated values of T_{iso}. The results obtained for the isokinetic temperature by application of five different methods are compiled in Table 2.

Table 2 Values of the dispersion factor and isokinetic temperature obtained by different methods[a]

Method	F_{iso} (%)[b]	T_{iso} / K[b]
1[c]	—	542 ± 43
2[d]	—	572 ± 104
3[e]	2.06 ± 0.31	560 ± 41
4[f]	1.97 ± 0.15	559 ± 44
5[g]	2.06 ± 0.17	560 ± 44

[a] For the oxidation of a series of eight *m*- and *p*-substituted cinnamic acids by tributylmethylammonium permanganate in methylene chloride solutions

[b] F_{iso} stands for the dispersion factor corresponding to the experimental value of the isokinetic temperature (T_{iso})

[c]Method 1: from the slope of the $\Delta H^{o}_{\neq,i}$ vs. $\Delta S^{o}_{\neq,i}$ experimental linear plot

[d]Method 2: from the ratio of the slopes of the $\Delta H^{o}_{\neq,i}$ vs. σ_i and $\Delta S^{o}_{\neq,i}$ vs. σ_i experimental linear plots

[e]Method 3: from the T_{iso} vs. $E(T_{iso})$ maximum probability curve

[f]Method 4: from the T_{iso} vs. r maximum probability curve

[g]Method 5: from the T_{iso} vs. E_{iso} maximum probability curve.

We can see that the methods numbered as 3, 4 and 5 yielded very similar, consistent results. These methods allowed discounting the decreasing effect provoked by the dispersion of the activation parameters on the experimental isokinetic temperature, thus leading to the most probable value of this

magnitude. Since that dispersion affected more to the entropies than to the enthalpies (Fig. 2), it could not be entirely due to random experimental errors (according to which the imprecisions of $\Delta H^{o}_{\neq,i}$ and $\Delta S^{o}_{\neq,i}$ would be closely related [35–37]) but to the own nature of each reaction of the homologous series.

Effect of experimental random errors: a critical appreciation

It has been much discussed whether the enthalpy-entropy compensation effect is caused by a physically meaningful phenomenon or it is just an artifact provoked by the interconnected experimental errors affecting the thermodynamic parameters [30–34]. In order to test this, the deviations of the enthalpies, $\delta(\Delta H^{o}_{\neq,i})$, and entropies, $\delta(\Delta S^{o}_{\neq,i})$, of activation from the respective $\Delta H^{o}_{\neq,i}$ vs. σ_i and $\Delta S^{o}_{\neq,i}$ vs. σ_i straight lines were calculated and represented in a $\delta(\Delta H^{o}_{\neq,i}) - \delta(\Delta S^{o}_{\neq,i})$ diagram for the reactions of *t*-butyl nitrite with *m*- and *p*-substituted phenols in dimethyl formamide solutions (Fig. 9) [61].

It can be observed that the deviations of the enthalpy increased linearly with those of the entropy, the slope (T_δ) being dimensionally a temperature. This and other statistical parameters were systematically analyzed for 10 homologous reaction series searched in the chemical literature [59–64].

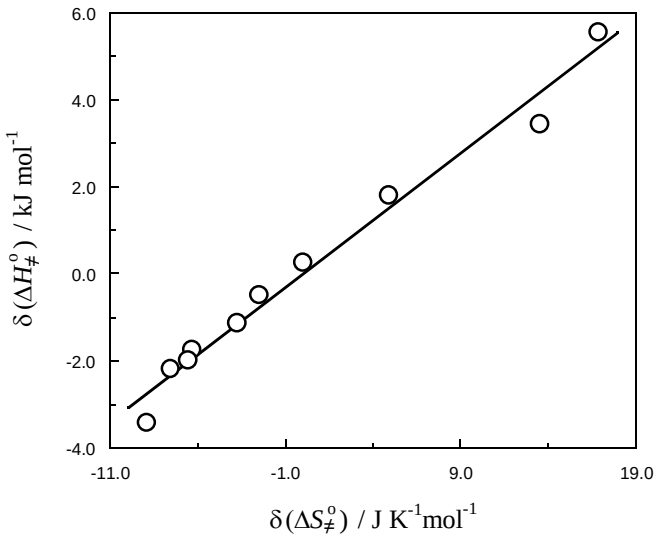

Fig. 9 Deviations of the activation enthalpies from the $\Delta H^{o}_{\neq,i}$ vs. σ_i straight line as a function of the deviations of the activation entropies from the $\Delta S^{o}_{\neq,i}$ vs. σ_i straight line for the reactions of *t*-butyl nitrite with a series of ten *m*- and *p*-substituted phenols in dimethyl formamide solutions (r = 0.990)

Since it has been demonstrated [35–37] that the random errors of the activation enthalpy are directly proportional to those of the entropy, according to the equation:

$$e(\Delta H^{o}_{\neq,i}) = T_m\, e(\Delta S^{o}_{\neq,i}) \qquad (19)$$

where T_m is the mean working temperature, we can conclude that the smaller the differences $D(1) = \left| T_{iso} - T_m \right|$ and $D(2) = \left| T_{\delta} - T_m \right|$ the smaller should be our confidence in the experimental values of the isokinetic temperature,

because they are very much contaminated by the random errors committed in the laboratory (Table 3).

Table 3 Statistical kinetic data for ten homologous reaction series from the chemical literature

T_m[a] / K	T_{iso}[a] / K	T_δ[b] / K	D_1[c] / K	D_2[c] / K	Reference
286	542	220	256	66	59
308	450	333	142	25	60
313	293	267	20	46	61
313	340	336	27	23	61
313	355	308	42	5	61
313	376	360	63	47	61
313	333	324	20	11	61
312	334	315	22	3	62
311	372	387	61	76	63
303	353	339	50	36	64

[a] The values of T_m and T_{iso} are the mean working and isokinetic temperatures for each reaction series

[b] The values of T_δ are the slopes of the $\delta(\Delta H^{o}_{\neq,i})$ vs. $\delta(\Delta S^{o}_{\neq,i})$ linear plots

[c] $D(1)$ and $D(2)$ stand for the absolute values of the $T_{iso} - T_m$ and $T_\delta - T_m$ differences, respectively

Table 4 Values of the correlation coefficients for the linear plots corresponding to ten homologous reaction series from the chemical literature

$\Delta H^{o}_{\neq}$ vs. σ	$\Delta S^{o}_{\neq}$ vs. σ	log k_{298} vs. σ	$\Delta H^{o}_{\neq}$ vs. $\Delta S^{o}_{\neq}$	$\delta(\Delta H^{o}_{\neq})$ vs. $\delta(\Delta S^{o}_{\neq})$	Reference
0.991	0.956	0.986	0.981	0.858	59
0.984	0.971	0.988	0.998	0.999	60
0.870	0.868	0.849	0.999	0.989	61
0.803	0.726	0.918	0.989	0.997	61
0.727	0.700	0.763	0.995	0.990	61
0.548	0.343	0.805	0.965	0.992	61
0.391	0.316	0.802	0.996	0.999	61
0.964	0.959	0.987	1.000	0.999	62
0.972	0.974	0.959	1.000	0.998	63
0.982	0.981	0.982	1.000	0.998	64

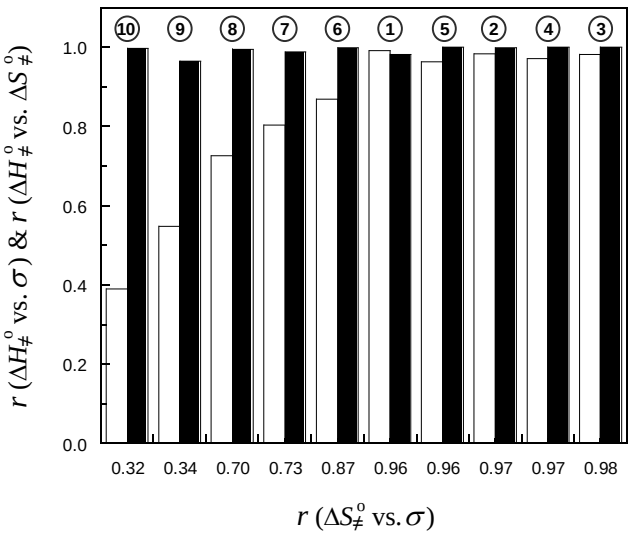

Fig. 10 Correlation coefficients for the $\Delta H^{o}_{\neq,i}$ vs. σ_i (white bars) and $\Delta H^{o}_{\neq,i}$ vs. $\Delta S^{o}_{\neq,i}$ (black bars) linear plots as a function of those for the $\Delta S^{o}_{\neq,i}$ vs. σ_i linear plots. The circled numbers indicate the order of confidence of the respective enthalpy-entropy isokinetic plots

Moreover, a correlation coefficient of the $\Delta H^{o}_{\neq,i}$ vs. $\Delta S^{o}_{\neq,i}$ linear plot much higher than those obtained for the $\Delta H^{o}_{\neq,i}$ vs. σ_i and $\Delta S^{o}_{\neq,i}$ vs. σ_i plots should also be taken as strongly indicative of the experimental value of T_{iso} being too much error driven (Table 4 and Fig. 10).

Conclusion

(i) The linear correlations of both the LFER (log k_T vs. σ_i) and isokinetic ($\Delta H^{o}_{\neq,i}$ vs. $\Delta S^{o}_{\neq,i}$) types often found in chemical kinetics for different homologous reaction series seem to be direct consequences of two other linear correlations: $\Delta H^{o}_{\neq,i}$ vs. σ_i and $\Delta S^{o}_{\neq,i}$ vs. σ_i, where σ_i is the Hammett (or Taft) substituent parameter. (ii) The LFER-type straight lines at different temperatures for a given homologous reaction series cross each other at a common intersection point, corresponding to a hypothetical member of the series with zero activation energy (E_a = 0). (iii) The Arrhenius (log k_T vs. $1/T$) or Eyring (log k_T/T vs. $1/T$) straight lines for different members of a homologous reaction series cross each other at a

common intersection point, corresponding to the temperature at which the reaction constant of the series takes a zero value (ρ = 0), so that the electronic effects of the substituents do not affect the reaction rate. (iv) A correlation coefficient of the $\Delta H^{o}_{\neq,i}$ vs. $\Delta S^{o}_{\neq,i}$ linear plot much higher than those of the $\Delta H^{o}_{\neq,i}$ vs. σ_i and $\Delta S^{o}_{\neq,i}$ vs. σ_i plots is indicative of a false isokinetic relationship, highly contaminated by experimental random errors.

Methods

Random number generator

In some of the programs needed to perform the numerical simulations, a set of scattered numbers was required (to simulate the potentially accidental character of some enthalpy-entropy data, as well as to incorporate the random errors involved in all experimental determinations). To this purpose, a random number generator was included in one of the subroutines, starting with the square root of a non-perfect square number, the scattered values being then taken from the successive decimal digits, and a random positive or negative sign was ascribed depending on the nature of the first digit (even or odd).

Calculations and graphics

The linear fits were performed by means of the least square method. The hardware used in all the numerical simulations and figures was a Sony Vaio personal computer. The software employed for the calculations was the programming language BBC BASIC (version for Windows) and for the graphics the program KaleidaGraph (version 4.03).

References

1. Gonzalez G, Lahuerta P, Martinez M, Peris E, Sanau M (1994) J Chem Soc Dalton Trans 545
2. Perez-Benito JF, Martinez-Cereza G (2018) J Phys Chem A 122:7962
3. Bhooshan M, Rajanna KC, Govardhan D, Venkanna P, Kumar MS (2019) Int J Chem Kinet 51:445
4. Vlasov VM (2018) Monatsh Chem 149:2161
5. Petersen RC, Markgraf JH, Ross SD (1961) J Am Chem Soc 83:3819
6. Leffler JE (1955) J Org Chem 20:1202
7. Akhtar MA, Li CZ (2020) Fuel 263:116632
8. Cao HQ, Duan QL, Chai H, Li XX, Sun JH (2020) J Hazard Mater 384:121297
9. Linert W (1987) Chem Phys 114:457

10. Sugihara G, Shigematsu DS, Nagadome S (2000) Langmuir 16:1825
11. Davidovits P, Jayne JT, Duan SX, Wornsop DR, Zahinser MS, Kolb CE (1991) J Phys Chem 95:6337
12. Nathanson GM, Davidovits P, Wornsop DR, Kolb CE (1996) J Phys Chem 100:13007
13. Chen YF, Pu WF, Li YB, Liu XL, Jin FY, Hui J, Gong XL, Guo C. (2018) Energy Fuels 32:12308
14. Shimakawa K, Aniya M (2013) Monatsh Chem 144:67
15. Sagotra AK, Chu D, Cazorla C (2019) Phys Rev Mater 3:035405
16. Sedivy L, Belas E, Grill R, Musiienko A, Vasylchenko I (2019) J Alloys Compd 788:897
17. Wang LF, Sun B, Liu HF, Lin DY, Song HF (2019) J Nucl Mater 526:151762
18. Crine JP (2013) Monatsh Chem 144:11
19. Crandall RS (1991) Phys Rev B 43:4057
20. Srivastava A, Sharma SD, Metha N (2018) Ceram Int 44:20827
21. Engstrom O (2013) Monatsh Chem 144:73
22. Rosenberg B, Bhowmik BB, Harder HC, Postow E (1968) J Chem Phys 49:4108
23. Ashraf IM, El-Zahhar AA (2018) Results Phys 11:842

24. He Q, Xu X, Gu Y, Cheng X, Xu J, Jiang Y (2018) ACS Appl Nano Mater 1:6959
25. Kumar A, Mehta N (2018) J Phys Chem Solids 121:49
26. Biswas D, Singh LS, Das AS, Bhattacharya S (2019) J Non-Cryst Solids 510:101
27. Braun A, Chen Q, Yelon A (2019) Chimia 73:936
28. Wojcik NA, Kupracz P, Barczynski RJ (2019) Solid State Ion 341:115055
29. Moyano PC, Zuñiga RN (2004) J Food Eng 63:57
30. McBane GC. (1998) J Chem Educ 75:919
31. Sharp K (2001) Prot Sci 10:661
32. Cornish-Bowden A (2002) J Biosci 27:121
33. Starikov EB, Norden B (2007) J Phys Chem B 111:14431
34. Cornish-Bowden A (2017) J Biosci 42:665
35. Krug RR, Hunter WG, Grieger RA (1976) Nature 261:566
36. Krug RR, Hunter WG, Grieger RA (1976) J Phys Chem 80:2335
37. Krug RR, Hunter WG, Grieger RA (1976) J Phys Chem 80:2341
38. Barrie PJ (2012) Phys Chem Chem Phys 14:318
39. Perez-Benito JF (2013) Monatsh Chem 144:49
40. Barrie PJ (2012) Phys Chem Chem Phys 14:327
41. Koudriavtsev AB, Linert W (2013) Match-Commun Math Co 70:7

42. Perez-Benito JF, Mulero-Raichs M (2016) J Phys Chem A 120:7598
43. Liu L, Guo QX (2001) Chem Rev 101:673
44. Keane MA, Larsson R (2009) Catal Lett 129:93
45. Keane MA, Larsson R (2012) React Kinet Mech Catal 106:267
46. Larsson R (2013) Monatsh Chem 144:21
47. Larsson R (2015) Molecules 20:2529
48. Larsson R (2018) Catalysts 8:97
49. Yelon A, Movaghar B, Crandall RS (2006) Rep Prog Phys 69:1145
50. Yelon A, Sacher E, Linert W (2011) Catal Lett 141:954
51. Abdel-Wahab F, Yelon A (2013) J Appl Phys 114:023707
52. Yelon A (2017) MRS Adv 2:425
53. Linert W (1986) Aust J Chem 39:199
54. Linert W, Sapunov VN (1988) Chem Phys 119:265
55. Harifi-Mood AR, Khorshahi H (2019) Int J Chem Kinet 51:511
56. Meadows MK, Sun XL, Kolesnichenko IV, Hinson CM, Johnson KA, Anslyn EV (2019) Chem Sci 10:8817
57. Perez-Benito JF, Lee DG (1987) J Org Chem 52:3239
58. Oh H, Ching WM, Kim J, Lee WZ, Hong S (2019) Inorg Chem 58:12964
59. Perez-Benito JF (1987) Chem Scr 27:433

60. El Guesmi N, Boubaker T, Goumont R (2010) Int J Chem Kinet 42:203
61. Kumar MS, Rajanna KC, Venkateswarlu M, Rao KL (2016) Int J Chem Kinet 48:171
62. Srinivas P, Suresh M, Rajanna KC, Krishnaiah G (2017) Int J Chem Kinet 49:209
63. Manjari PS, Suresh M, Reddy CS (2011) Transition Met Chem 36:707
64. Manjunatha AS, Dakshayani S, Vaz N, Puttaswamy (2016) Korean J Chem Eng 33:697

Fig. Captions

Fig. 1 Simulated plots for a second-order homologous reaction series with the activation energies (0, 10, 20, 30 and 40) kJ mol^{-1} at the temperatures (10, 20, 30, 40 and 50) ºC. Top: Hammett or Taft plots (the circles correspond to the different activation energies and the straight lines to the temperatures). Bottom: Eyring plots (the circles correspond to the different temperatures and the straight lines to the activation energies)

Fig. 2 Experimental enthalpies (r = 0.991, top) and entropies (r = 0.956, bottom) of activation as a function of the Hammett σ parameter for the oxidation of a series of eight *m*- and *p*-substituted cinnamic acids by tributylmethylammonium permanganate in methylene chloride solutions

Fig. 3 Experimental values of the Hammett reaction constant as a function of the reciprocal absolute temperature for the oxidation of a series of eight *m*- and *p*-substituted cinnamic acids by tributylmethylammonium permanganate in methylene chloride solutions (T_{iso} = 542 K, top) and the S_NAr reactions of a series of five *m*- and *p*-substituted anilines with 2,6-bis(trifluoromethanesulfonyl)-4-nitroanisole in methanol solutions (T_{iso} = 450 K, bottom), showing the extrapolation required to reach the respective isokinetic temperatures (ρ = 0)

Fig. 4 Linear correlation coefficients associated with the $\log k_{298,\mathrm{i}}$ vs σ_{i} (top) and $\Delta H^{\mathrm{o}}_{\neq,\mathrm{i}}$ vs. $\Delta S^{\mathrm{o}}_{\neq,\mathrm{i}}$ (bottom) plots as a function of the dispersion factor from simulations based on the oxidation of a series of eight *m*- and *p*-substituted cinnamic acids by tributylmethylammonium permanganate in methylene chloride solutions, assuming that only either the entropies (left) or the enthalpies (right) of activation were dispersed, showing the scattered points found when the simulations were performed just once and the maximum probability curves found when the simulations were performed 10^6 times for each *F* value

Fig. 5 Linear correlation coefficients associated with the $\Delta H^{\mathrm{o}}_{\neq,\mathrm{i}}$ vs. σ_{i} (a), $\Delta S^{\mathrm{o}}_{\neq,\mathrm{i}}$ vs. σ_{i} (b), $\log k_{298,\mathrm{i}}$ vs. σ_{i} (c) and $\Delta H^{\mathrm{o}}_{\neq,\mathrm{i}}$ vs. $\Delta S^{\mathrm{o}}_{\neq,\mathrm{i}}$ (d) plots as a function of the percent dispersion factor from numerical simulations based on the oxidation of a series of eight *m*- and *p*-substituted cinnamic acids by tributylmethylammonium permanganate in methylene chloride solutions, showing the maximum probability curves found when the simulations were performed 10^4 times for each *F* value. Inset: detail showing the range *F* = 0 – 8 %

Fig. 6 Top: double logarithm plots of the probability of the $\Delta H^{o}_{\neq,i}$ vs. $\Delta S^{o}_{\neq,i}$ and $\log k_{298,i}$ vs. σ_i relationships being simultaneously linear as a function of the probability of the $\log k_{298,i}$ vs. σ_i relationship considered alone being linear. Bottom: double logarithm plots of the probability of the $\log k_{298,i}$ vs. σ_i and $\Delta H^{o}_{\neq,i}$ vs. $\Delta S^{o}_{\neq,i}$ relationships being simultaneously linear as a function of the probability of the $\Delta H^{o}_{\neq,i}$ vs. $\Delta S^{o}_{\neq,i}$ relationship considered alone being linear. From 10^6 numerical simulations performed for each *F* value, based on the cinnamic acid reaction series, with dispersion factor values in the range $F = 0.0 - 7.2$ % and correlation coefficients higher than 0.90, 0.92, 0.94, 0.96 and 0.98 (in upward order). The dashed lines correspond to a condition for which the two probabilities would be identical

Fig. 7 Logarithm of the probability of the slopes (ρ or T_{iso}) and average ordinate fitting errors (E_{Ham} or E_{iso}) corresponding to the $\log k_{298,i}$ vs. σ_i (a), $\Delta H^{o}_{\neq,i}$ vs. $\Delta S^{o}_{\neq,i}$ (b) or both (c) linear plots being within ± 10 % of the experimental values as a function of the percent dispersion factor, with only the activation entropies scattered, from 10^6 numerical simulations for each *F* value and based on the oxidation of a series of eight *m*- and *p*-substituted cinnamic

acids by tributylmethylammonium permanganate in methylene chloride solutions

Fig. 8 Isokinetic temperature as a function of either its standard deviation (top), the correlation coefficient (middle) or the average ordinate fitting error (bottom) found when the simulations were performed 10^6 times for each dispersion factor value (in the range F = 0 – 100 %) with only the entropies scattered, and based on the oxidation of a series of eight *m*- and *p*-substituted cinnamic acids by tributylmethylammonium permanganate in methylene chloride solutions, showing the maximum probability curves starting at either T_{iso} = (518, 560 and 601) K (top), T_{iso} = (515, 559 and 603) K (middle) or T_{iso} = (516, 561 and 605) K (bottom), as well as the experimental points (filled circles) and their error-tolerated limits (empty circles)

Fig. 9 Deviations of the activation enthalpies from the $\Delta H^{o}_{\neq,i}$ vs. σ_i straight line as a function of the deviations of the activation entropies from the $\Delta S^{o}_{\neq,i}$ vs. σ_i straight line for the reactions of *t*-butyl nitrite with a series of ten *m*- and *p*-substituted phenols in dimethyl formamide solutions (r = 0.990)

Fig. 10 Correlation coefficients for the $\Delta H^{o}_{\neq,i}$ vs. σ_i (white bars) and $\Delta H^{o}_{\neq,i}$ vs. $\Delta S^{o}_{\neq,i}$ (black bars) linear plots as a function of those for the $\Delta S^{o}_{\neq,i}$ vs. σ_i linear plots. The circled numbers indicate the order of confidence of the respective enthalpy-entropy isokinetic plots

Table 1 Coordinates of the probability curve maxima[a]

Linear plot	$F_{max,1}$ (%)[b]	$P_{max,1}$[b]	$F_{max,2}$ (%)[c]	$P_{max,2}$[c]	$F_{max,3}$ (%)[d]	$P_{max,3}$[d]
Hammett	1.41	0.263	1.62	0.226	1.12	0.230
Isokinetic	1.88	0.230	3.70	0.192	1.66	0.220
Hammett-Isokinetic	1.56	0.007	–	–	1.80	0.003

[a]From 10^6 numerical simulations for each F value, based on the oxidation of a series of eight *m*- and *p*-substituted cinnamic acids by tributylmethylammonium permanganate in methylene chloride solutions. F_{max} and P_{max} are the abscissa and ordinate values corresponding to the maxima of the probability curves

[b]Method 1: only the activation entropies scattered

[c] Method 2: only the activation enthalpies scattered (P_2 = 0 for the combined Hammett-isokinetic probability curve at all F values)

[d]Method 3: both activation parameters scattered

Table 2 Values of the dispersion factor and isokinetic temperature obtained by different methods[a]

Method	F_{iso} (%)[b]	T_{iso} / K[b]
1[c]	–	542 ± 43
2[d]	–	572 ± 104
3[e]	2.06 ± 0.31	560 ± 41
4[f]	1.97 ± 0.15	559 ± 44
5[g]	2.06 ± 0.17	560 ± 44

[a] For the oxidation of a series of eight *m*- and *p*-substituted cinnamic acids by tributylmethylammonium permanganate in methylene chloride solutions

[b] F_{iso} stands for the dispersion factor corresponding to the experimental value of the isokinetic temperature (T_{iso})

[c] Method 1: from the slope of the $\Delta H^{o}_{\neq,i}$ vs. $\Delta S^{o}_{\neq,i}$ experimental linear plot

[d] Method 2: from the ratio of the slopes of the $\Delta H^{o}_{\neq,i}$ vs. σ_i and $\Delta S^{o}_{\neq,i}$ vs. σ_i experimental linear plots

[e] Method 3: from the T_{iso} vs. $E(T_{iso})$ maximum probability curve

[f] Method 4: from the T_{iso} vs. r maximum probability curve

[g] Method 5: from the T_{iso} vs. E_{iso} maximum probability curve.

Table 3 Statistical kinetic data for ten homologous reaction series from the chemical literature

T_m[a] / K	T_{iso}[a] / K	T_δ[b] / K	D_1[c] / K	D_2[c] / K	Reference
286	542	220	256	66	59
308	450	333	142	25	60
313	293	267	20	46	61
313	340	336	27	23	61
313	355	308	42	5	61
313	376	360	63	47	61
313	333	324	20	11	61
312	334	315	22	3	62
311	372	387	61	76	63
303	353	339	50	36	64

[a]The values of T_m and T_{iso} are the mean working and isokinetic temperatures for each reaction series

[b]The values of T_δ are the slopes of the $\delta(\Delta H^{o}_{\neq,i})$ vs. $\delta(\Delta S^{o}_{\neq,i})$ linear plots

[c] $D(1)$ and $D(2)$ stand for the absolute values of the $T_{iso} - T_m$ and $T_\delta - T_m$ differences, respectively

Table 4 Values of the correlation coefficients for the linear plots corresponding to ten homologous reaction series from the chemical literature

$\Delta H^{o}_{\neq}$ vs. σ	$\Delta S^{o}_{\neq}$ vs. σ	log k_{298} vs. σ	$\Delta H^{o}_{\neq}$ vs. $\Delta S^{o}_{\neq}$	$\delta(\Delta H^{o}_{\neq})$ vs. $\delta(\Delta S^{o}_{\neq})$	Reference
0.991	0.956	0.986	0.981	0.858	59
0.984	0.971	0.988	0.998	0.999	60
0.870	0.868	0.849	0.999	0.989	61
0.803	0.726	0.918	0.989	0.997	61
0.727	0.700	0.763	0.995	0.990	61
0.548	0.343	0.805	0.965	0.992	61
0.391	0.316	0.802	0.996	0.999	61
0.964	0.959	0.987	1.000	0.999	62
0.972	0.974	0.959	1.000	0.998	63
0.982	0.981	0.982	1.000	0.998	64

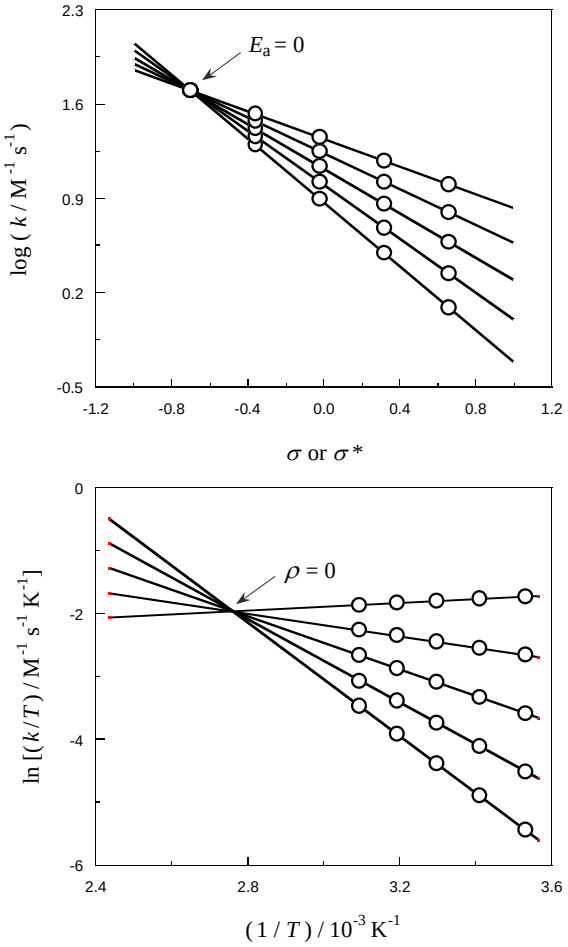

Fig. 1

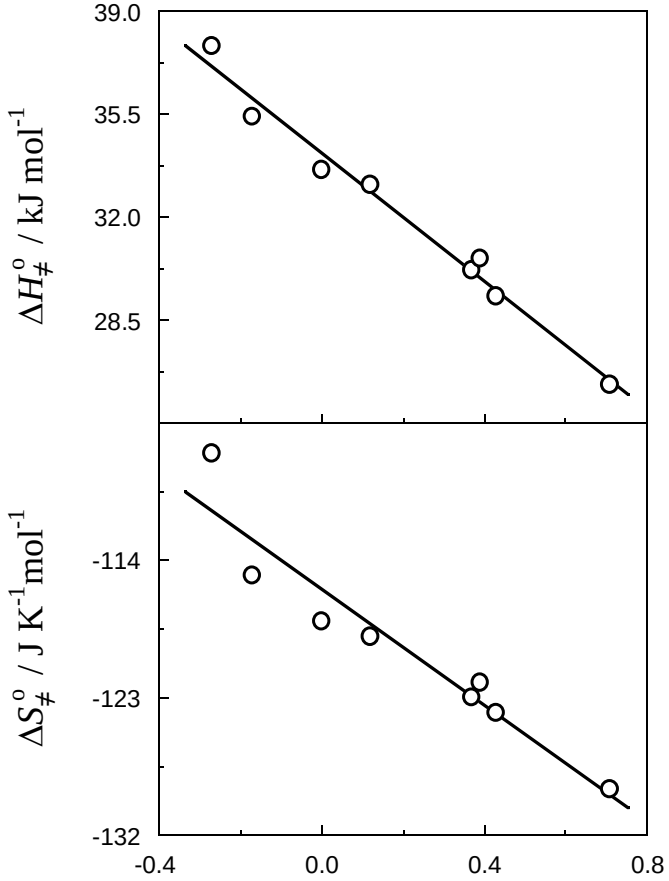
39.0
35.5
32.0
28.5
$\Delta H^{o}_{\neq}$ / kJ mol^{-1}
-114
-123
-132
$\Delta S^{o}_{\neq}$ / J K^{-1}mol^{-1}
-0.4
0.0
0.4
0.8
σ

Fig. 2

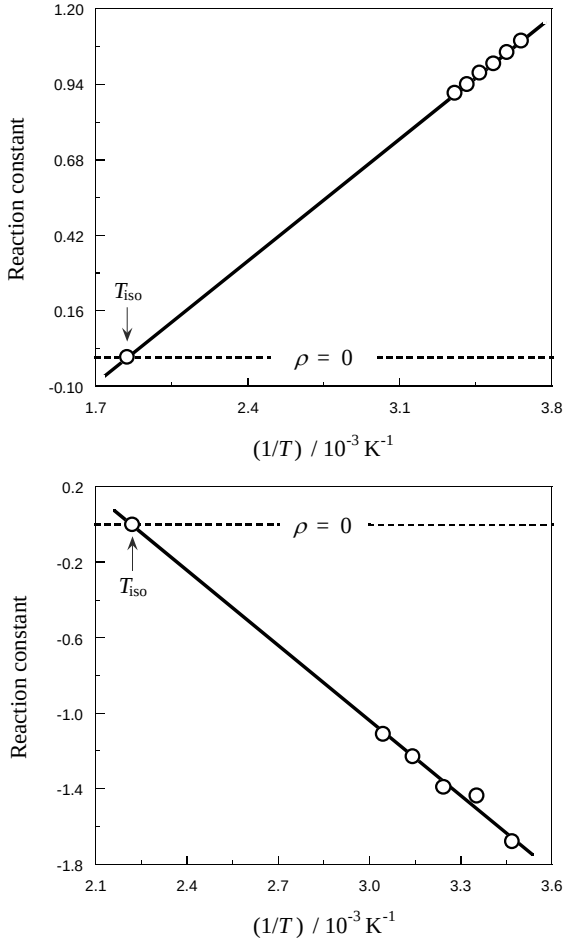
1.20
0.94
0.68
0.42
0.16
-0.10
Reaction constant
T_{iso}
ρ = 0
1.7
2.4
3.1
3.8
$(1/T)$ / 10^{-3} K^{-1}
0.2
-0.2
-0.6
-1.0
-1.4
-1.8
Reaction constant
ρ = 0
T_{iso}
2.1
2.4
2.7
3.0
3.3
3.6
$(1/T)$ / 10^{-3} K^{-1}

Fig. 3

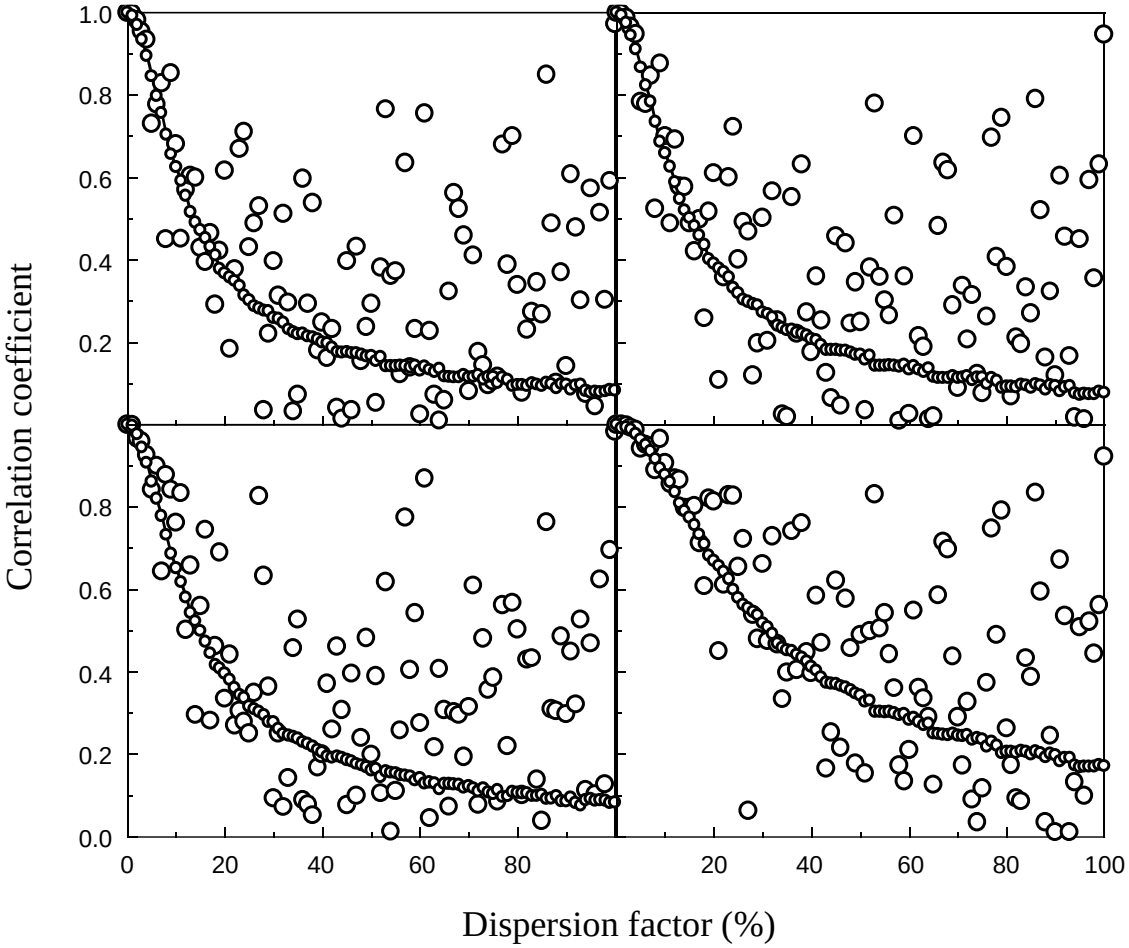
Correlation coefficient
Dispersion factor (%)
1.0
0.8
0.6
0.4
0.2
0.0
0
20
40
60
80
100

Fig. 4

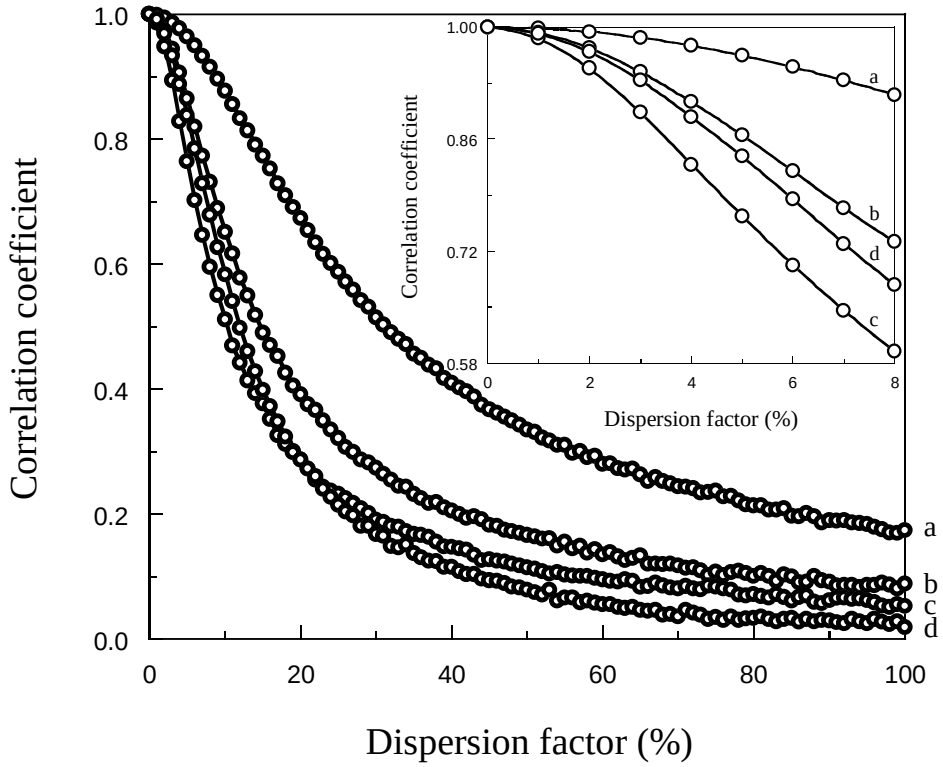
Correlation coefficient
1.0
0.8
0.6
0.4
0.2
0.0
0
20
40
60
80
100
Dispersion factor (%)
a
b
c
d
Correlation coefficient
1.00
0.86
0.72
0.58
0
2
4
6
8
Dispersion factor (%)
a
b
d
c

Fig. 5

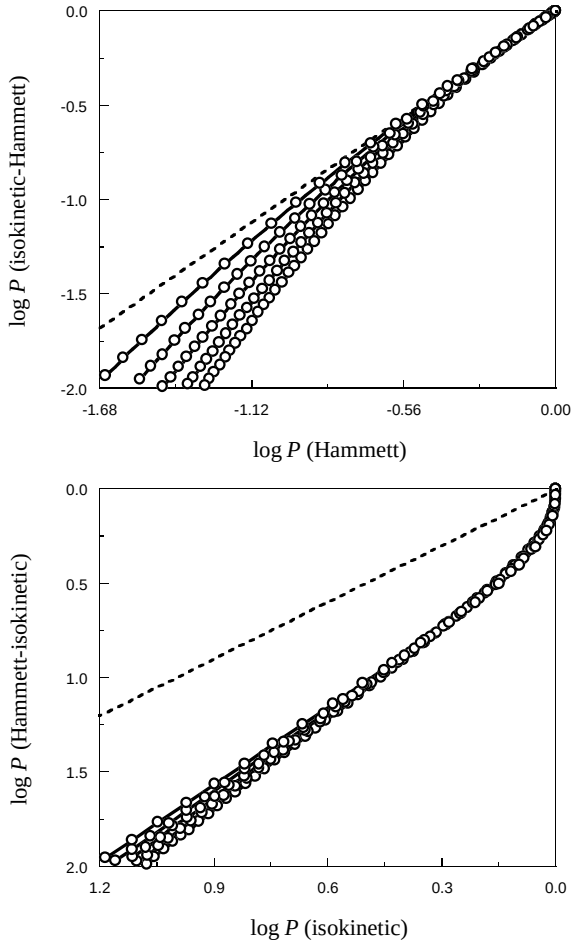
0.0
-0.5
-1.0
-1.5
-2.0
log P (isokinetic-Hammett)
-1.68
-1.12
-0.56
0.00
log P (Hammett)
0.0
0.5
1.0
1.5
2.0
log P (Hammett-isokinetic)
1.2
0.9
0.6
0.3
0.0
log P (isokinetic)

Fig. 6

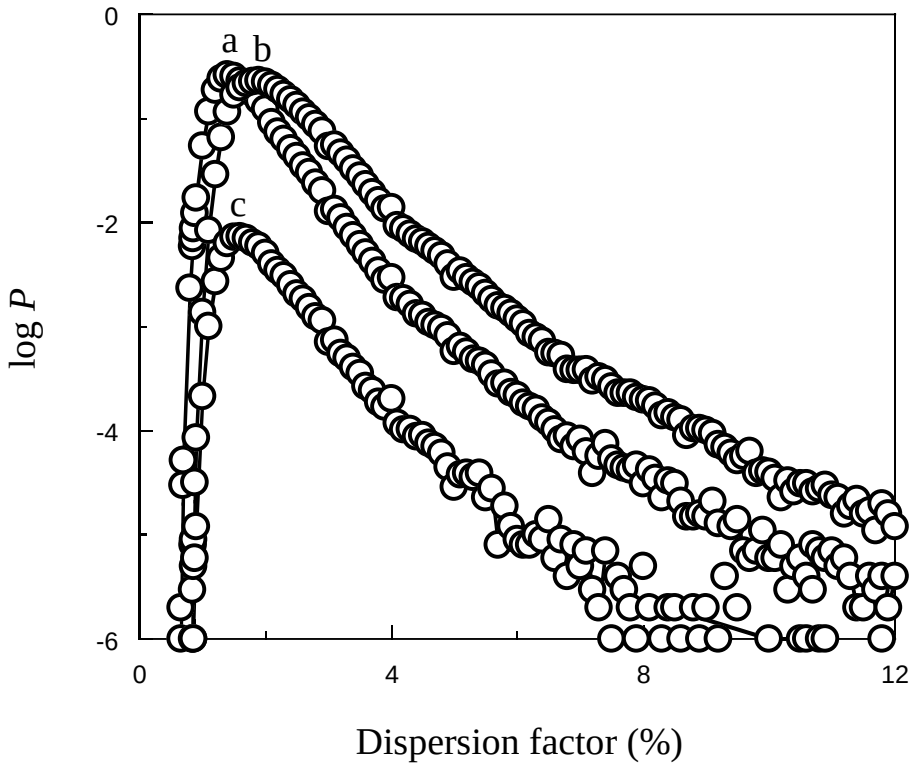

Fig. 7

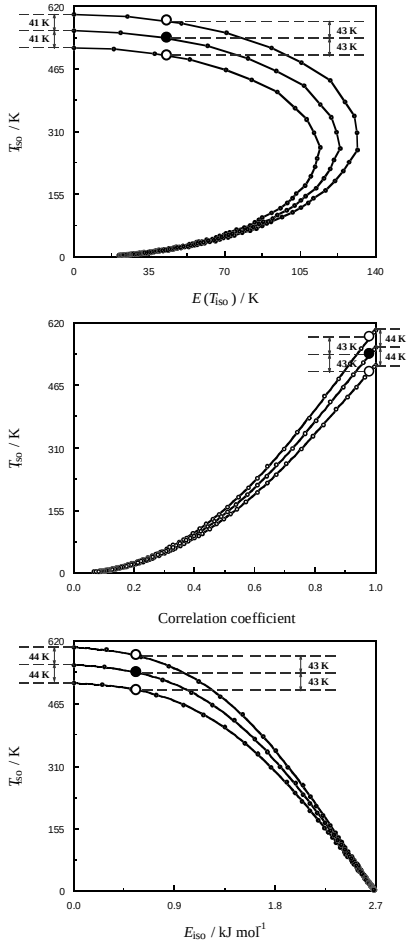
41 K
41 K
43 K
43 K
T_{iso} / K
$E(T_{iso})$ / K
43 K
43 K
44 K
44 K
Correlation coefficient
44 K
44 K
43 K
43 K
E_{iso} / kJ mol^{-1}

Fig. 8

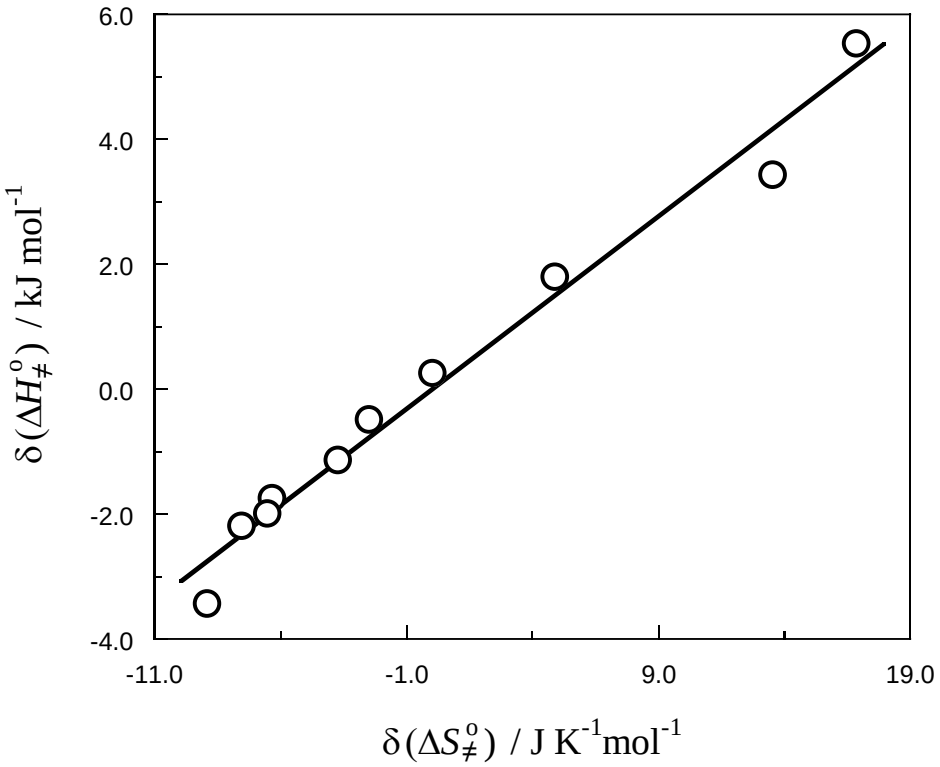
6.0
4.0
2.0
0.0
-2.0
-4.0
-11.0
-1.0
9.0
19.0
$\delta(\Delta H_{\neq}^{o})$ / kJ mol^{-1}
$\delta(\Delta S_{\neq}^{o})$ / J K^{-1}mol^{-1}

Fig. 9

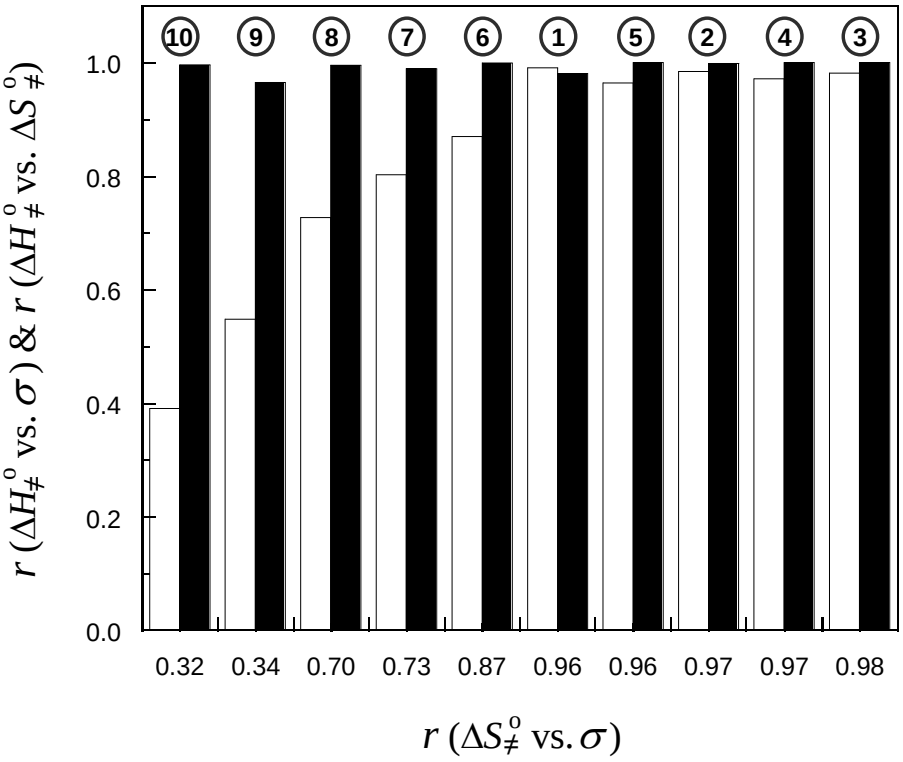
10
9
8
7
6
1
5
2
4
3
1.0
0.8
0.6
0.4
0.2
0.0
0.32
0.34
0.70
0.73
0.87
0.96
0.96
0.97
0.97
0.98
$r\ (\Delta H_{\neq}^{o}\ \text{vs.}\ \sigma)\ \&\ r\ (\Delta H_{\neq}^{o}\ \text{vs.}\ \Delta S_{\neq}^{o})$
$r\ (\Delta S_{\neq}^{o}\ \text{vs.}\ \sigma)$

Fig. 10

Graphical abstract